NANO LETTERS

2009
Vol. 9, No. 9
3312-3317

Carbon Nanotubes Activate Blood Platelets by Inducing Extracellular Ca^{2+} Influx Sensitive to Calcium Entry Inhibitors

Jana Semberova,[†,‡] Silvia H. De Paoli Lacerda,[†] Olga Simakova,[||] Karel Holada,[§] Monique P. Gelderman,[†] and Jan Simak*[,†]

Center for Biologics Evaluation and Research, Food and Drug Administration, Rockville, Maryland 20852-1448, Institute for the Care of Mother and Child, Prague, Czech Republic, First Medical School, Charles University, Prague, Czech Republic, and NIH Clinical Center, Bethesda, Maryland 20892

Received May 20, 2009; Revised Manuscript Received July 6, 2009

ABSTRACT

To elucidate a mechanism of prothrombotic effects of carbon nanotubes (CNTs), we report here that multiwalled CNTs activate blood platelets by inducing extracellular Ca^{2+} influx that could be inhibited by calcium channel blockers SKF 96365 and 2-APB. We also demonstrate platelet aggregating activity of different single-walled and multiwalled CNTs. In addition, we show that CNT-induced platelet activation is associated with a marked release of platelet membrane microparticles positive for the granular secretion markers CD62P and CD63.

Carbon nanotechnology has developed very rapidly over the past years resulting in an ever-increasing production of various types of carbon nanotubes (CNTs). Their unique mechanical, thermal, and electronic properties make CNTs very attractive candidates for numerous biomedical applications.[1] Several examples are diagnostic biosensors, drug delivery nanosystems, imaging nanoprobes for intravascular use and other devices that come in direct contact with blood. Also, the number of industrial facilities producing the CNTs for a relatively low cost has increased and therefore, the chance of occupational and environmental exposure has increased as well.[2] Different nanomaterials have been shown to penetrate through the skin[3,4] and pass across epithelia of other organs,[5,6] which might ultimately lead to their presence intravascularly. Although interaction of nanomaterials with biological systems has been extensively studied[7] and several international standard biocompatibility assays are currently under development,[8,9] the information addressing the potential hazard related to CNTs exposure is still up for debate.[10−15] Only a very few studies exploring CNTs in contact with intravascular environment and components of circulating blood, particularly platelets, have been published so far.[16,17] In addition, mechanisms of CNT effects on platelets have not been elucidated. Here we show that CNTs induce platelet activation, aggregation and the release of platelet membrane microparticles via facilitated extracellular Ca^{2+} influx. We found that CNT-induced Ca^{2+} influx is sensitive to calcium entry blockers SKF 96365 and 2-APB, indicating involvement of store-operated calcium entry (SOCE).

We have studied the effects of structurally diverse purified CNTs on human platelets (PLTs) and compared their effects to amorphous carbon nanopowder (ACN), C_{60} fullerene (nC60), fullerenol (C60(OH)24), and standard polystyrene nanobeads (PBs). Carbon nanomaterials were purchased from various manufacturers and their purity ranged from 90−99% (Table 1). We confirmed the purity and the structure of all tested materials by transmission electron microscopy (TEM) analysis (see Supporting Information). In order to study interactions of pristine CNTs, amorphous carbon, and C_{60} fullerene with platelets, these materials were tested as polydisperse suspensions prepared by minimal sonication to allow platelet contacts with material surface but to avoid its chemical changes. In our experiments, materials were resuspended to a concentration of 1 mg/mL in phosphate buffered saline and sonicated immediately prior to use for 1 min at 30 W output, frequency 20 kHz (Tekmar Sonic Disruptor, Cincinnati, OH). To characterize nanomaterial agglomerates at our experimental conditions, the flow particle image analysis of nanomaterial suspensions in plasma was

* To whom correspondence should be addressed. E-mail: jan.simak@fda.hhs.gov. Tel: 301-827-3978. Fax: 301-402-2780.
[†] Food and Drug Administration.
[‡] Institute for the Care of Mother and Child.
[||] NIH Clinical Center.
[§] Charles University.

10.1021/nl901603k CCC: $40.75
Published on Web 07/28/2009

Table 1. List of Tested Carbon Nanomaterials[a]

nanomaterial	abbrev	manufacturer	minimal purity	outer diameter	length	platelet aggregation activity
amorphous carbon nanopowder	ACN	Sigma-Aldrich	>99%	~ 30 nm	N/A	+
SWCNT	S1	SES	>90%	<2 nm	5−15 μm	+++
SWCNT	S2	NanoAmor	>95%	1−2 nm	5−30 μm	+++
MWCNT	M60	SES	>95%	60−100 nm	1−2 μm	+++
MWCNT	M30	NanoLab	>95%	30 ± 15 nm	1−5 μm	+++
Fullerene C60	nC60	MER	99.9%	~0.7 nm	N/A	-
Fullerenol C60	C60(OH)24	MER	N/A	~1.3 nm	N/A	-
standard polystyrene nanobeads	PB20	Duke Scientific	N/A	20 nm	N/A	-
	PB200	Duke Scientific	N/A	200 nm	N/A	-

[a] Semiquantitative evaluation of platelet aggregating activity. Maximum platelet aggregation 0−5%, -; 6−15%, +; 16−25%, ++; >25%, +++. All materials were tested at concentration 100 μg/mL. MWCNT, multiwalled carbon nanotubes; SWCNT, single-walled carbon nanotubes; N/A, not available.

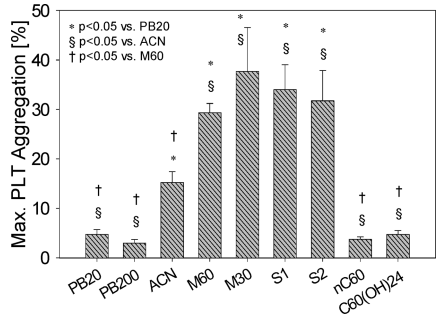

Figure 1. Comparison of platelet aggregating activity of tested carbon nanomaterials. Significant difference from standard polystyrene nanobeads (*), amorphous carbon nanopowder (§) and M60 (†) is shown ($p < 0.05$, mean of 5 experiments ± SEM). See Table 1 for abbreviations.

performed using FPIA 3000 (Sysmex, Kobe, Japan, provided by Malvern Instruments, Columbia, MD). The analysis showed that nanomaterials formed polydisperse agglomerates of a median size 0.7−2.7 μm, depending on the type of nanomaterial: nC60 median CE diameter 0.7 μm (10−90th percentile = 0.4−1.5 μm), M60 MWCNT 1.4 μm (0.5−8.3 μm), amorphous carbon ACN 2.8 μm (0.5−10.0 μm). We also confirmed that the tested materials (M60, ACN, nC60) did not progressively agglomerate in plasma during a period of 30 min, an incubation period used for testing of effects on platelets (see Supporting Information).

To assess the effect of carbon nanotubes on platelet aggregation, we employed light transmission aggregometry (PAP-8E aggregometer, Bio/Data Corp., Horsham, PA). Platelet rich plasma (PRP) was prepared from blood of healthy donors (acid citrate dextrose anticoagulated, Department of Transfusion Medicine, Clinical Center, NIH, Bethesda, MD). Aggregation experiments were completed within 4 h after blood collection to ensure normal platelet responsiveness. Each experiment was performed using at least three blood samples from different donors. Means of maximum aggregation responses ± standard error of mean (SEM) are presented. All tested CNTs showed significant PLT aggregation activity in PRP (Figure 1). At the tested concentration 100 μg/mL, the single-walled carbon nanotubes (SWCNTs) S1 showed maximum PLT aggregation 34 ± 5%, similar to S2 (32 ± 6%) and both multiwalled carbon nanotubes (MWCNTs) M60 (27 ± 3%) and M30 (38 ± 9%), which was significantly higher compared to ACN (15 ± 2%). In contrast, fullerene nC60, fullerenol C60(OH)24, or polystyrene nanobeads (PBs) did not cause any significant PLT aggregation. Collagen was used as a positive control (100%) for each experiment. For further experiments, we selected MWCNTs with a 60 nm diameter, M60, as a representative CNT material due to its purity and highly reproducible platelet aggregating performance. The M60 concentration dependent PLT aggregation response is shown in Figure 2A. Since all commercial CNTs contain variable levels of contaminants, particularly heavy metals that can leach into the solution, we tested a potential effect of leachables from M60 material on platelets. When the CNT agglomerates were sedimented at 20 000 g (10 min; 20 °C) from the suspension of M60 1 mg/ mL, the supernatant did not induce platelet aggregation (not shown). This result indicates that the CNT agglomerates >0.4 μm observed by FPIA analysis were responsible for M60-induced platelet aggregating activity and that the effect of potential leaching was not significant.

While investigating the mechanism of CNT-induced platelet aggregation, we questioned the role of calcium. Our study has focused on effects of CNTs on intracellular free Ca^{2+} concentration $[Ca^{2+}]_i$ in platelets since Ca^{2+} is a key second messenger controlling critical steps in platelet activation, such as reorganization of cytoskeleton which leads to the shape change, degranulation and platelet aggregation. Thus, the increase of $[Ca^{2+}]_i$ is essential for platelet activation in hemostasis and thrombosis.[18] Platelets elevate $[Ca^{2+}]_i$ by releasing Ca^{2+} from two intracellular stores, dense tubular system and lysosome-like acidic organelles.[19] Another way to increase $[Ca^{2+}]_i$ is to facilitate Ca^{2+} entry through plasma membrane channels. Performing the experiments in an environment with a different Ca^{2+} content showed that the CNT-induced platelet aggregation response is proportional to the extracellular Ca^{2+} concentration (Figure 2B). This finding led us to hypothesize that CNTs induce platelet activation by facilitating extracellular Ca^{2+} influx. In platelets, Ca^{2+} may enter through the plasma membrane by different mechanisms. These include receptor-operated Ca^{2+} entry, second messenger-operated Ca^{2+} entry, and store-operated Ca^{2+} entry (SOCE).[19] The possibility of a nonspecific disintegration of plasma membrane should also be considered.

To characterize the CNT-induced Ca^{2+} influx, we employed inhibitors of platelet calcium signaling pathways. We found that M60-induced platelet aggregation was suppressed

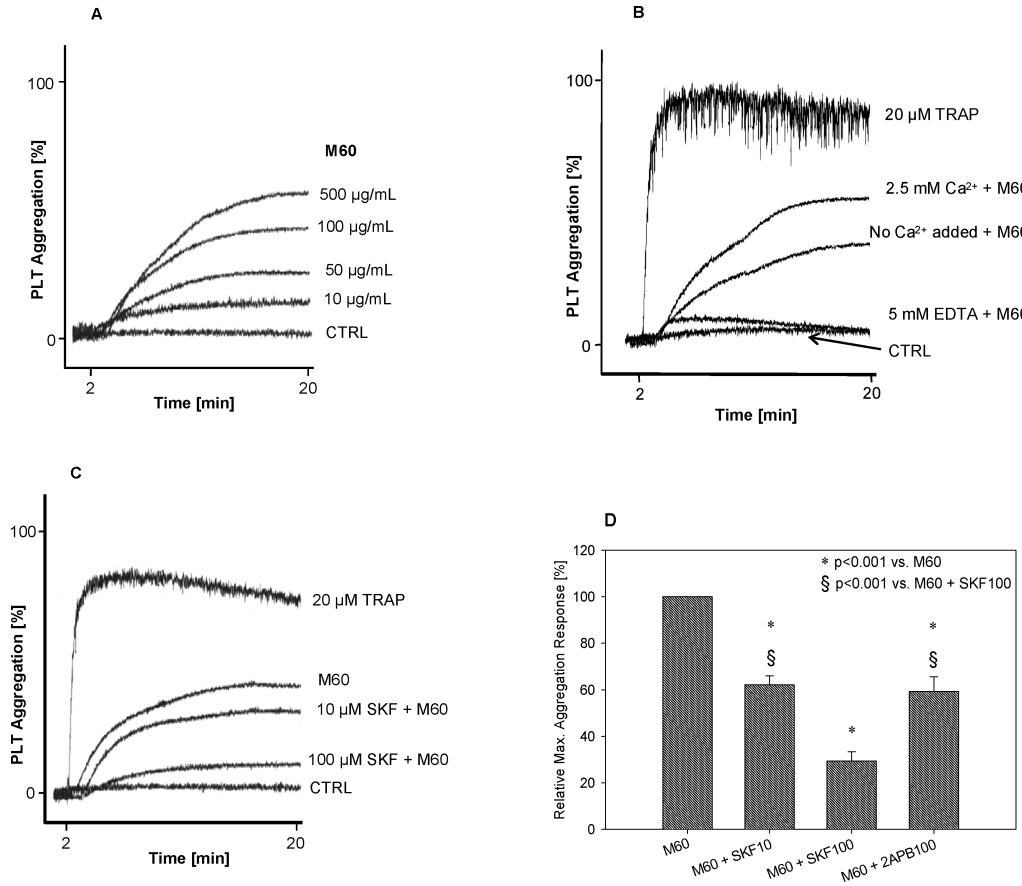

Figure 2. Platelet aggregation induced by multiwalled carbon nanotubes M60. (A) M60 concentration-dependent PLT aggregation response. (B) PLT aggregation response induced by M60 (100 μg/mL) was proportional to the extracellular Ca^{2+} concentration. (C) Calcium entry blocker SKF 96365 inhibited PLT aggregation induced by M60 (100 μg/mL) in a dose dependent manner. PRP with 1 IU/mL heparin and 2.5 mM Ca^{2+} was used if not otherwise indicated. Representative traces of the light transmission aggregometry experiments ($n = 3$) are shown. The bar graph (D) shows inhibition of M60-induced platelet aggregation with 10 μM SKF 96365 (M60 + SKF10), 100 μM SKF 96365 (M60 + SKF100), and 100 μM 2-APB (M60 + 2APB100) compared to M60 control without inhibitor (M60). Means + SEM ($n = 5$) of relative maximum aggregation response are shown. 2APB, 2-aminoethoxydiphenyl borate; CTRL, control platelets treated with vehicle only; CNT, carbon nanotubes; EDTA, ethylenediaminetetraacetic acid; M60, multiwalled carbon nanotubes with outer diameter 60 nm; PLT, platelets; PRP, platelet rich plasma; SKF, SKF 96365 (1-[2-(4-methoxyphenyl)-2-[3-(4-methoxyphenyl)propoxy]ethyl]imidazole hydrochloride); TRAP, thrombin receptor activating peptide.

with calcium channel blockers SKF 96365 (1-[2-(4-methoxyphenyl)-2-[3-(4-methoxyphenyl)propoxy]ethyl]imidazole) and 2-APB (2-aminoethoxydiphenyl borate) (Figure 2B,C). This result indicates involvement of SOCE. While SKF 96365 has overlapping effects on SOCE and receptor-operated calcium entry, 2-APB has more specific activities, including direct extracellular inhibition of SOCE channels.[20−25] In contrast, no effect on M60-induced PLT aggregation response was observed with DM-BAPTA AM (40 μM; membrane permeant intracellular Ca^{2+} chelator), NF 449 (1 μM; P2X1 blocker), MRS 2500 (5 nM; P2Y1 blocker), or TBHQ (20 μM; SERCA3 blocker) (data not shown).

In order to confirm the CNT-induced extracellular Ca^{2+} influx in platelets, we investigated the acute effect of CNTs on intracellular free Ca^{2+} concentration $[Ca^{2+}]_i$ in individual platelets loaded with a Ca^{2+}-sensitive probe FURA-2 AM employing ratio fluorometry.[26] Changes in fluorescence in individual platelets ($n = 100$) were monitored at 340 and 380 nm excitation, using a Nikon inverted epi-fluorescence/phase microscope equipped with a low-light level integrating CCD camera with a microphotometer assembly (InCyt I/P-2 TM Imaging and Photometry System, Intracellular Imaging Inc., Cincinnati, OH). Real time $[Ca^{2+}]_i$ was calculated from the ratio of emission detected at 510 nm at two excitation wavelengths (340 and 380 nm) and by comparison to a standard curve established for these settings using buffers of known free Ca^{2+}.

We demonstrated that M60 induced a rapid concentration-dependent increase in platelet $[Ca^{2+}]_i$ indicative of Ca^{2+} entry (Figure 3). The increase of $[Ca^{2+}]_i$ above base level was 90 $\pm$ 4 nM immediately upon addition of M60. In contrast, after administration of 100 μg/mL ACN or PBs no changes in $[Ca^{2+}]_i$ were detected. Also, there was no response to M60 observed in experiments conducted in a calcium free condition, confirming the extracellular origin of Ca^{2+} (data not shown). Moreover, in agreement with the platelet aggregation experiment results, no Ca^{2+} influx was observed when platelets were pretreated with 10 μM calcium entry blocker SKF 96365 (Figure 3).

SOCE, also called capacitative calcium entry (CCE), is a biphasic Ca^{2+} signaling process, where release of Ca^{2+} from

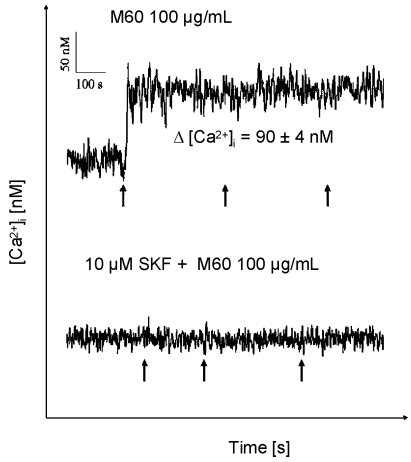

Figure 3. M60-induced rapid elevation of intracellular calcium in platelets as measured by ratio fluorometry of PLT loaded with FURA-2AM. Ca^{2+} influx could be completely inhibited with 10 μM SKF 96365 (10 min preincubation). There was no increase in $[Ca^{2+}]_i$ observed in PLT treated with ACN or PB, neither with M60 in Ca^{2+} free conditions (data not shown). Response of 100 PLT was evaluated in each experiment ($n = 3$). A representative tracing of responding PLTs from one experiment is shown. Arrows indicate the addition of M60 (100 μg/mL final conc. per dose). PLT, platelets; M60, multiwalled carbon nanotubes with outer diameter 60 nm; PB, standard polystyrene nanobeads; ACN, amorphous carbon nanopowder; SKF, SKF 96365 (1-[2-(4-methoxyphenyl)-2-[3-(4-methoxyphenyl)propoxy]ethyl]imidazole hydrochloride).

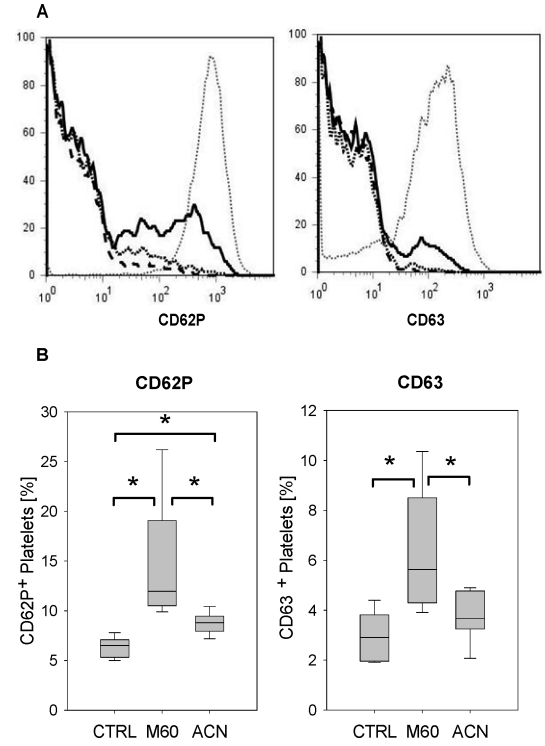

Figure 4. Flow cytometry analysis of platelet surface activation markers. Representative histograms of five experiments are shown (A). M60 (solid line) induced a slight but significant increase in the platelet surface expression of CD62P and CD63 compared to amorphous carbon nanopowder (dotted line) and nontreated platelets (dashed line). 20uM TRAP was used as a positive control (gray dotted line). Percentage of $CD62P^+$ and $CD63^+$ platelets is shown on box and whiskers plots (B) indicating the median (full line), the 25−75th and the 10−90th percentiles of the group distribution as boxes and error bars, respectively ($n = 5$); * $p < 0.05$. M60, multiwalled carbon nanotubes with outer diameter 60 nm; ACN, amorphous carbon nanopowder; CTRL, control platelets treated with vehicle only; TRAP, thrombin receptor activating peptide.

intracellular storage (endoplasmatic reticulum, dense tubular system in platelets) is followed by the Ca^{2+} entry across the platelet plasma membrane.[22,27,28] It has been shown recently that a plasma membrane ion channel protein ORAI1 mediates the interaction between stromal interaction molecule STIM1 and the transient receptor potential channel protein hTRPC1 and thus regulates the mode of activation of hTRPC1-forming Ca^{2+} channels.[29] Therefore, it is likely that the STIM1-ORAI1-hTRPC1 complex plays a key functional role in SOCE activation. Further investigation should elucidate whether and how CNTs interact with this complex and stimulate SOCE activation. Although both calcium entry blockers 2-APB and SKF 96365 significantly inhibited M60-induced PLT aggregation, none of them abolished the response completely, indicating a complex nature of the CNT-induced PLT aggregation response. Also, the participation of a noncapacitative mechanism of the CNT-induced Ca^{2+} entry cannot be excluded. The specificity of the tested calcium entry inhibitors for SOCE channels is disputable, however the fact is that we were able to inhibit CNT-induced Ca^{2+} influx using these compounds. This indicates that the Ca^{2+} influx is not caused by unspecific physical perforation of the platelet membrane but rather by specific interactions of CNTs with membrane structures, cytoskeleton, receptors, and/or channel proteins. These results warrant further investigation on a molecular level.

To further characterize CNT-induced PLT activation, we investigated PLT surface exposure of activation markers CD62P and CD63 using flow cytometry.[30] CD62P (P-selectin) is expressed in resting platelets on the membrane of platelet α-granules and it is exposed on the platelet surface after α-granule secretion. It is believed that the activation dependent increase in platelet surface P-selectin exposure is not reversible over time in vitro.[31] However, P-selectin may be released from the platelet surface in a soluble or membrane microparticle (MP) associated form. CD63 is another degranulation dependent platelet surface marker that in resting platelets resides on the membranes of the lysosomes and dense granules.[32] Thus, the platelet surface exposure of CD63 requires stronger activation signal compared to CD62P. In our experiments, platelets were stimulated with M60 (100 μg/mL) for 15 min at 37 °C with a gentle agitation. Platelets treated with 20 μM TRAP or PBs were used as a positive and negative control, respectively. For flow cytometric analysis, platelet surface markers were labeled with fluorescent monoclonal antibodies, CD41a (FITC labeled) and CD62P or CD63 respectively (both PE labeled). Data were acquired using a FACSCalibur flow cytometer (Becton Dickinson, San Diego, CA) equipped with CELLQuest software with forward scatter and side scatter in logarithmic mode and subsequently analyzed using FlowJo (Tree Star, Inc. Ashland, OR). Expression of platelet activation markers was evaluated as a percentage of $CD62P^+$ and $CD63^+$ platelets.

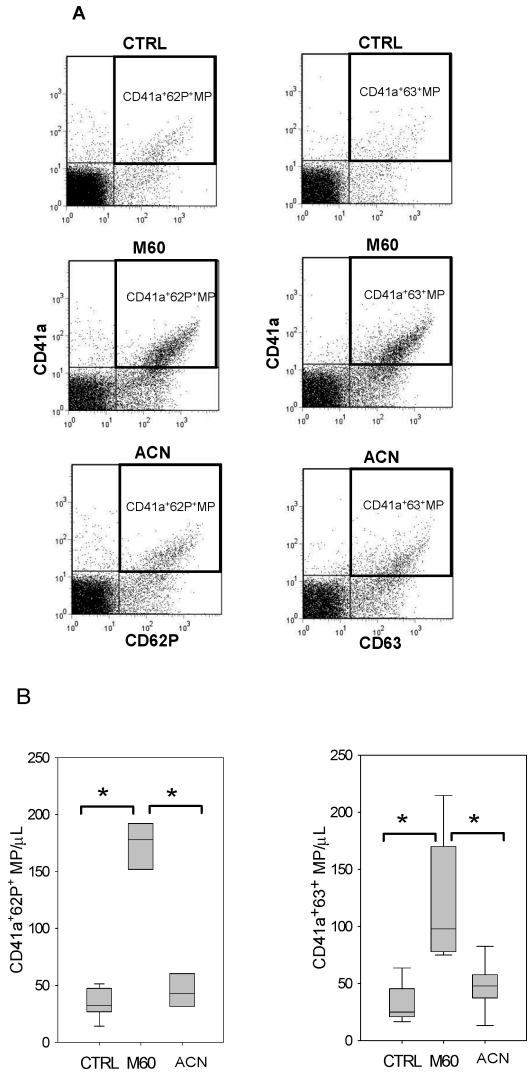

Figure 5. Flow cytometry analysis of platelet membrane microparticles. M60 induced significant release of $CD41a^+CD62P^+$ and $CD41a^+CD63^+$ platelet membrane microparticles compared to ACN and CTRL. Representative double fluorescence dot plots (A) of five experiments show gated MP positive for $CD41a^+CD62P^+$ and $CD41a^+CD63^+$, respectively. Counts of released $CD41a^+CD62P^+$-MP and $CD41a^+CD63^+$MP are shown on box and whiskers plots (B) indicating the median (full line), the 25−75th and the 10−90th percentiles of the group distribution as boxes and error bars, respectively ($n = 5$); * $p < 0.05$. M60, multiwalled carbon nanotubes with outer diameter 60 nm; ACN, amorphous carbon nanopowder; CTRL, control platelets treated with vehicle only; MP, microparticles.

M60-induced PLT activation led to significantly higher surface exposure of CD62P and CD63 compared to ACN and untreated platelets. Also, CD62P expression after treatment with ACN differed significantly from untreated platelets (Figure 4). Increase in the surface exposure of CD62P and CD63 on M60-stimulated platelets was not as high as expected. Therefore we investigated whether these antigens were released from platelet surface in membrane microparticles. Membrane microparticles (MPs) are phopholipid vesicles of about 0.1−1 μm in size released from plasma membrane of stimulated platelets and other cell types.[33] Platelet MPs expose various platelet membrane antigens and a majority of platelet MPs also expose phosphatidylserine, thus being procoagulant and may be prothrombotic in vivo. We analyzed MPs by flow cytometry as described previously.[34,35]

Platelet MP assays and platelet surface marker analysis were run in parallel, using identical blood specimen, both types of samples were stained with the same type of fluorescent monoclonal antibodies. MPs were defined as particles ≤1 μm in size compared to forward scatter with the size standard polystyrene beads of 1 μm in diameter. Counts of $CD41a^+CD62P^+$MPs and $CD41a^+CD63^+$MPs in the platelet supernatant was evaluated using double fluorescence plots (Figure 5A) acquired for 60 s at the standard flow rate determined by TruCount (BD) beads. MP count per microliter of PRP was calculated. Interestingly, in contrast to ACN, M60 induced a marked release of $CD41a^+CD62P^+$MPs and $CD41a^+CD63^+$MPs (Figure 5B). Strong platelet MP releasing activity of CNTs may contribute to CNT prothrombotic effects observed in the arterial thrombosis model in rats.[16]

Taken together, our results demonstrate that CNTs activate human platelets by inducing extracellular Ca^{2+} influx, which is susceptible to SOCE inhibitors 2-APB and SKF 96365. Thus, CNTs induce platelet aggregation and marked release of platelet membrane microparticles positive for alpha granular and dense granular/lysosomal membrane proteins. This study represents a true multidisciplinary approach integrating nanotechnology with cell biology, where the mechanism of platelet activation with characterized CNT materials has been studied. Our results warrant further investigations to completely understand and elucidate a mechanism of CNT-induced Ca^{2+} influx in platelets. The observed findings are significant since understanding a mechanism of prothrombotic and other blood and vascular toxic effects of CNTs is critical in the development of biocompatible CNT materials for biomedical use, as well as for evaluation of widely discussed health risk of CNTs in environmental and occupational exposure.

Acknowledgment. We thank Gerald Sando, Ph.D., Malvern Instruments, Columbia, MD, for the flow particle image analysis of nanomaterial suspensions. K.H. was supported by grant MSM 0021620806 of the Ministry of Education, Youth, and Sport of the Czech Republic. The findings and conclusions in this article have not been formally disseminated by the Food and Drug Administration and should not be construed to represent any Agency determination or policy.

Supporting Information Available: Materials and methods, including TEM analysis of the tested nanomaterials and FPIA analysis of nanomaterial suspensions in plasma, details on platelet aggregation assay, platelet intracellular Ca^{2+} assay, and flow cytometry analysis of platelet surface activation markers and platelet microparticles are provided. This material is available free of charge via the Internet at http://pubs.acs.org.

References

(1) Baughman, R. H.; Zakhidov, A. A.; de Heer, W. A. Carbon nanotubes--the route toward applications. *Science* **2002**, *297* (5582), 787–92.

(2) Colvin, V. L. The potential environmental impact of engineered nanomaterials. *Nat. Biotechnol.* **2003**, *21* (10), 1166–70.
(3) Rouse, J. G.; Yang, J.; Ryman-Rasmussen, J. P.; Barron, A. R.; Monteiro-Riviere, N. A. Effects of mechanical flexion on the penetration of fullerene amino acid-derivatized peptide nanoparticles through skin. *Nano Lett* **2007**, *7* (1), 155–60.
(4) Ryman-Rasmussen, J. P.; Riviere, J. E.; Monteiro-Riviere, N. A. Penetration of intact skin by quantum dots with diverse physicochemical properties. *Toxicol. Sci.* **2006**, *91* (1), 159–65.
(5) Berry, J. P.; Arnoux, B.; Stanislas, G.; Galle, P.; Chretien, J. A microanalytic study of particles transport across the alveoli: role of blood platelets. *Biomedicine* **1977**, *27* (9−10), 354–7.
(6) Nemmar, A.; Hoet, P. H.; Vanquickenborne, B.; Dinsdale, D.; Thomeer, M.; Hoylaerts, M. F.; Vanbilloen, H.; Mortelmans, L.; Nemery, B. Passage of inhaled particles into the blood circulation in humans. *Circulation* **2002**, *105* (4), 411–4.
(7) Oberdorster, G.; Maynard, A.; Donaldson, K.; Castranova, V.; Fitzpatrick, J.; Ausman, K.; Carter, J.; Karn, B.; Kreyling, W.; Lai, D.; Olin, S.; Monteiro-Riviere, N.; Warheit, D.; Yang, H. Principles for characterizing the potential human health effects from exposure to nanomaterials: elements of a screening strategy. *Part. Fibre Toxicol.* **2005**, *2*, 8.
(8) Dobrovolskaia, M. A.; Clogston, J. D.; Neun, B. W.; Hall, J. B.; Patri, A. K.; McNeil, S. E. Method for analysis of nanoparticle hemolytic properties in vitro. *Nano Lett.* **2008**, *8* (8), 2180–7.
(9) Hall, J. B.; Dobrovolskaia, M. A.; Patri, A. K.; McNeil, S. E. Characterization of nanoparticles for therapeutics. *Nanomedicine* **2007**, *2* (6), 789–803.
(10) Lam, C. W.; James, J. T.; McCluskey, R.; Hunter, R. L. Pulmonary toxicity of single-wall carbon nanotubes in mice 7 and 90 days after intratracheal instillation. *Toxicol. Sci.* **2004**, *77* (1), 126–34.
(11) Lam, C. W.; James, J. T.; McCluskey, R.; Arepalli, S.; Hunter, R. L. A review of carbon nanotube toxicity and assessment of potential occupational and environmental health risks. *Crit. Rev. Toxicol.* **2006**, *36* (3), 189–217.
(12) Shvedova, A. A.; Castranova, V.; Kisin, E. R.; Schwegler-Berry, D.; Murray, A. R.; Gandelsman, V. Z.; Maynard, A.; Baron, P. Exposure to carbon nanotube material: assessment of nanotube cytotoxicity using human keratinocyte cells. *J. Toxicol. Environ. Health, Part A* **2003**, *66* (20), 1909–26.
(13) Magrez, A.; Kasas, S.; Salicio, V.; Pasquier, N.; Seo, J. W.; Celio, M.; Catsicas, S.; Schwaller, B.; Forro, L. Cellular toxicity of carbon-based nanomaterials. *Nano Lett.* **2006**, *6* (6), 1121–5.
(14) Dumortier, H.; Lacotte, S.; Pastorin, G.; Marega, R.; Wu, W.; Bonifazi, D.; Briand, J. P.; Prato, M.; Muller, S.; Bianco, A. Functionalized carbon nanotubes are non-cytotoxic and preserve the functionality of primary immune cells. *Nano Lett.* **2006**, *6* (7), 1522–8.
(15) Medina, C.; Santos-Martinez, M. J.; Radomski, A.; Corrigan, O. I.; Radomski, M. W. Nanoparticles: pharmacological and toxicological significance. *Br. J. Pharmacol.* **2007**, *150* (5), 552–8.
(16) Radomski, A.; Jurasz, P.; Alonso-Escolano, D.; Drews, M.; Morandi, M.; Malinski, T.; Radomski, M. W. Nanoparticle-induced platelet aggregation and vascular thrombosis. *Br. J. Pharmacol.* **2005**, *146* (6), 882–93.
(17) Niwa, Y.; Iwai, N. Nanomaterials induce oxidized low-density lipoprotein cellular uptake in macrophages and platelet aggregation. *Circ. J.* **2007**, *71* (3), 437–44.
(18) Varga-Szabo, D.; Braun, A.; Nieswandt, B. Calcium signaling in platelets. *J. Thromb. Haemostasis* **2009**, *7* (7), 1057–66.
(19) Jardin, I.; Lopez, J. J.; Pariente, J. A.; Salido, G. M.; Rosado, J. A. Intracellular calcium release from human platelets: different messengers for multiple stores. *Trends Cardiovasc. Med.* **2008**, *18* (2), 57–61.
(20) Ben-Amor, N.; Redondo, P. C.; Bartegi, A.; Pariente, J. A.; Salido, G. M.; Rosado, J. A. A role for 5,6-epoxyeicosatrienoic acid in calcium entry by de novo conformational coupling in human platelets. *J. Physiol.* **2006**, *570* (Pt 2), 309–23.
(21) Diver, J. M.; Sage, S. O.; Rosado, J. A. The inositol trisphosphate receptor antagonist 2-aminoethoxydiphenylborate (2-APB) blocks Ca2+ entry channels in human platelets: cautions for its use in studying Ca2+ influx. *Cell Calcium* **2001**, *30* (5), 323–9.
(22) Bird, G. S.; DeHaven, W. I.; Smyth, J. T.; Putney, J. W., Jr. Methods for studying store-operated calcium entry. *Methods* **2008**, *46* (3), 204–12.
(23) Bootman, M. D.; Collins, T. J.; Mackenzie, L.; Roderick, H. L.; Berridge, M. J.; Peppiatt, C. M. 2-aminoethoxydiphenyl borate (2-APB) is a reliable blocker of store-operated Ca2+ entry but an inconsistent inhibitor of InsP3-induced Ca2+ release. *FASEB. J* **2002**, *16* (10), 1145–50.
(24) Marumo, M.; Wakabayashi, I. Monensin augments capacitative Ca2+ entry and subsequent aggregation of platelets via an intracellular alkalosis-mediated mechanism. *Pharmacol. Res.* **2005**, *51* (2), 141–5.
(25) Vostal, J. G.; Jackson, W. L.; Shulman, N. R. Cytosolic and stored calcium antagonistically control tyrosine phosphorylation of specific platelet proteins. *J. Biol. Chem.* **1991**, *266* (25), 16911–6.
(26) Simakova, O.; Arispe, N. J. The cell-selective neurotoxicity of the Alzheimer's Abeta peptide is determined by surface phosphatidylserine and cytosolic ATP levels. Membrane binding is required for Abeta toxicity. *J. Neurosci.* **2007**, *27* (50), 13719–29.
(27) Putney, J. W., Jr. Recent breakthroughs in the molecular mechanism of capacitative calcium entry (with thoughts on how we got here). *Cell Calcium* **2007**, *42* (2), 103–10.
(28) Rosado, J. A. Discovering the mechanism of capacitative calcium entry. *Am. J. Physiol. Cell Physiol.* **2006**, *291* (6), C1104−6.
(29) Jardin, I.; Lopez, J. J.; Salido, G. M.; Rosado, J. A. Orai1 mediates the interaction between STIM1 and hTRPC1 and regulates the mode of activation of hTRPC1-forming Ca2+ channels. *J. Biol. Chem.* **2008**, *283* (37), 25296–304.
(30) Simak, J.; Holada, K.; Janota, J.; Stranak, Z. Surface expression of major membrane glycoproteins on resting and TRAP-activated neonatal platelets. *Pediatr. Res.* **1999**, *46* (4), 445–9.
(31) Michelson, A. D. Evaluation of platelet function by flow cytometry. *Pathophysiol. Haemostasis Thromb.* **2006**, *35* (1−2), 67–82.
(32) Israels, S. J.; McMillan-Ward, E. M. Platelet tetraspanin complexes and their association with lipid rafts. *Thromb. Haemostasis* **2007**, *98* (5), 1081–7.
(33) Simak, J.; Gelderman, M. P. Cell membrane microparticles in blood and blood products: potentially pathogenic agents and diagnostic markers. *Transfusion Med. Rev.* **2006**, *20* (1), 1–26.
(34) Simak, J.; Gelderman, M. P.; Yu, H.; Wright, V.; Baird, A. E. Circulating endothelial microparticles in acute ischemic stroke: a link to severity, lesion volume and outcome. *J. Thromb. Haemostasis* **2006**, *4* (6), 1296–302.
(35) Gelderman, M. P.; Simak, J. Flow cytometric analysis of cell membrane microparticles. *Methods Mol. Biol.* **2008**, *484*, 79–93.

NL901603K